

Fuller

REPORT DOCUMENTATION PAGE

Form Approved
OMB No. 0704-0188

Public reporting burden for this collection of information is estimated to average 1 hour per response, including the time for reviewing instructions, searching existing data sources, gathering and maintaining the data needed, and completing and reviewing this collection of information. Send comments regarding this burden estimate or any other aspect of this collection of information, including suggestions for reducing this burden to Department of Defense, Washington Headquarters Services, Directorate for Information Operations and Reports (0704-0188), 1215 Jefferson Davis Highway, Suite 1204, Arlington, VA 22202-4302. Respondents should be aware that notwithstanding any other provision of law, no person shall be subject to any penalty for failing to comply with a collection of information if it does not display a currently valid OMB control number. PLEASE DO NOT RETURN YOUR FORM TO THE ABOVE ADDRESS.

1. REPORT DATE (DD-MM-YYYY) 20/12/2009	2. REPORT TYPE Final	3. DATES COVERED (From - To) 05/01/05-09/30/09
---	-------------------------	---

4. TITLE AND SUBTITLE Chemical Routes to Ceramics with Tunable Properties and Compositions: Chemical Routes to Nano and Micro-Structured Materials	5a. CONTRACT NUMBER
	5b. GRANT NUMBER FA9550-06-1-0228
	5c. PROGRAM ELEMENT NUMBER

6. AUTHOR(S) Larry G. Sneddon and Shu Yang	5d. PROJECT NUMBER
	5e. TASK NUMBER
	5f. WORK UNIT NUMBER

7. PERFORMING ORGANIZATION NAME(S) AND ADDRESS(ES) University of Pennsylvania Department of Chemistry 231 South 34 th Street Philadelphia, PA 19104-6323	8. PERFORMING ORGANIZATION REPORT NUMBER 9-2009
---	--

9. SPONSORING / MONITORING AGENCY NAME(S) AND ADDRESS(ES) Air Force Office of Scientific Research Ceramic and Nonmetallic Materials 801 N. Randolph Street, Room 732 Arlington, VA 22203-1977 Dr. Joan Fuller, Manager	10. SPONSOR/MONITOR'S ACRONYM(S) AFOSR
	11. SPONSOR/MONITOR'S REPORT NUMBER AFRL-OSR-VA-TR-2013-0922

12. DISTRIBUTION / AVAILABILITY STATEMENT
Publicly Available

13. SUPPLEMENTARY NOTES

14. ABSTRACT
The goal of this completed AFOSR research program was to design, synthesize and develop the materials applications of new processible chemical precursors to technologically important nonoxide ceramics that allow the formation of these ceramics in forms that have been unattainable with conventional methods. Major achievements include demonstrations that: (1) blends of boron and silicon-based preceramic polymers can be used as excellent precursors to boron-carbide/silicon-carbide ceramic composite materials in processed forms with certain compositions showing significant oxidation resistance, (2) chemical precursor systems composed of zirconium or hafnium powders dispersed into blends of boron and silicon preceramic polymers provide simple efficient routes to new types of complex ultra high temperature ZrB₂/ZrC/SiC and HfB₂/HfC/SiC composites, (3) blends of the Penn poly(norbornenyldecaborane) polymer with the commercial poly(methylcarbosilane) polymer could be electrostatically spun to produce polymer fibers that could then be thermally converted to nano- to micro-scale boron-carbide/silicon-carbide composite ceramic fibers, (4) silica-bead templating techniques employing preceramic polymers enable the generation of 2-dimensional nanoporous ceramic arrays, (5) diatom-templating methods provide excellent routes to micro- and nanostructured nonoxide ceramics, and (6) preceramic polymers can be used in conjunction with templates generated by multi-beam interference lithography to produce high temperature nonoxide ceramic photonic crystals.

15. SUBJECT TERMS
preceramics, photonic crystals, ceramics, silicon carbide, boron carbide, high temperature materials

16. SECURITY CLASSIFICATION OF:			17. LIMITATION OF ABSTRACT unlimited	18. NUMBER OF PAGES 17	19a. NAME OF RESPONSIBLE PERSON Larry G. Sneddon
a. REPORT unclassified	b. ABSTRACT unclassified	c. THIS PAGE unclassified			19b. TELEPHONE NUMBER (include area code) 215-898-8632

**CHEMICAL ROUTES TO CERAMICS WITH TUNABLE PROPERTIES AND
STRUCTURES: CHEMICAL ROUTES TO NANO AND MICRO-STRUCTURED
CERAMICS**

AFOSR GRANT FA9550-06-1-0228

Larry G. Sneddon and Shu Yang, Principal Investigators

Departments of Chemistry and Materials Science and Engineering
University of Pennsylvania
Philadelphia, Pennsylvania 19104-6323

December 2009

FINAL REPORT

Executive Summary

The goal of this research program was to design, synthesize and develop the materials applications of new processible chemical precursors to technologically important nonoxide ceramics that allow the formation of these ceramics in forms that have been unattainable with conventional methods. A second major goal of the project was to exploit the processibility of new precursor molecules and polymers in conjunction with newly established solid-state fabrication methods to achieve micro- and nano-structured ceramic materials. Major achievements include: (1) the demonstration that blends of boron and silicon-based preceramic polymers can be used as excellent precursors to boron-carbide/silicon-carbide ceramic composite materials in processed forms with certain compositions showing significant oxidation resistance, (2) the demonstration that chemical precursor systems composed of zirconium or hafnium powders dispersed into blends of boron and silicon preceramic polymers provide simple efficient routes to new types of complex ultra high temperature $ZrB_2/ZrC/SiC$ and $HfB_2/HfC/SiC$ composites, (3) the demonstration (in collaboration with Harry Allcock at Penn State) that blends of the Penn poly(norbornenyldecaborane) polymer with the commercial poly(methylcarbosilane) polymer could be electrostatically spun to produce polymer fibers that could then be thermally converted to nano- to micro-scale boron-carbide/silicon-carbide composite ceramic fibers, (4) the demonstration that silica-bead templating techniques employing preceramic polymers enable the generation of 2-dimensional nanoporous ceramic arrays, (5) the demonstration (in collaboration with Ken Sandhage at Georgia Tech) that diatom-templating methods provide excellent routes to micro- and nanostructured nonoxide ceramics, and (6) the demonstration that preceramic polymers can be used in conjunction with templates generated by multi-beam interference lithography to produce high temperature nonoxide ceramic photonic crystals.

CHEMICAL ROUTES TO CERAMICS WITH TUNABLE PROPERTIES AND STRUCTURES: CHEMICAL ROUTES TO NANO AND MICRO-STRUCTURED CERAMICS

AFOSR GRANT FA9550-06-1-0228

This research program was focused on the design, syntheses and applications of new processible chemical precursors to advanced ceramics, including boron-carbide, silicon-carbide and boron-carbide/silicon-carbide and ultra high temperature $ZrB_2/ZrC/SiC$ and $HfB_2/HfC/SiC$ composites that would allow the formation of these technologically important materials in forms, including especially nano- and micro-structural materials, that were unattainable with conventional methods. Major achievements are briefly discussed below:

Chemical Precursors to Complex Nonoxide Ceramic Composites

The unique properties of silicon-carbide and boron-carbide based ceramics give rise to numerous applications.^{1,2} Boron carbide has high chemical-inertness, thermal-stability and hardness, and excellent high-temperature thermoelectric properties, while silicon carbide is valued because of its low density, high strength, and excellent oxidation and thermal-shock resistance. Boron-carbide/silicon-carbide composites have likewise been shown to have enhanced properties relative to the individual ceramics. For example, while boron carbide oxidizes at ~ 600 °C to form B_2O_3 , boron-carbide/silicon-carbide composites have been reported to have oxidative stability up to 1200 °C as the result of the formation of a borosilicate glass layer that effectively blocks oxygen penetration.^{3,4,5}

Powder processing has been the most common method of making boron carbide and silicon carbide, but such methods are limited in their ability to produce ceramics in processed forms.⁶ More recently, processible polymeric precursors have been developed for both of these ceramics that allow their syntheses in more complex forms, including films and fibers. Nevertheless, the construction of similar single-source precursors for boron-carbide/silicon-carbide composite materials that would allow both for the formation of processed forms and easy tunability of composition would be a chemically difficult and expensive challenge. Our AFOSR sponsored project has demonstrated⁷ that simple blends of our poly(norbornenyldodecaborane) (PND)⁸ boron-carbide preceramic polymer with either of the commercial poly(methylcarbosilane) (PMCS) or allylhydridopolycarbosilane (AHPCS) silicon-carbide preceramic polymers provide excellent processible precursors to boron-carbide/silicon-carbide ceramic composite materials.

The ceramic chars obtained from the pyrolyses of PND/PMCS blends at different temperatures were consistent with the formation of $SiC/B_4C/C$ composites with the B_4C to SiC ratio in the ceramic increasing as the PND to PMCS ratio was increased in the precursor blend. Both boron-carbide and silicon-carbide crystallization was inhibited in the composites compared to the ceramics derived from the pure precursor polymers with materials pyrolyzed to only 1000 °C being amorphous. The onset of silicon carbide crystallization was apparent by XRD in the 1300 °C chars, but boron carbide diffraction only appeared after treatment at 1600 °C. As shown in Figure 1, TEM studies indicated that these ceramics were composed of nanocrystallites of silicon carbide embedded in an amorphous boron carbon matrix. The graphitic coating observed on the silicon carbide grains undoubtedly inhibited grain growth.

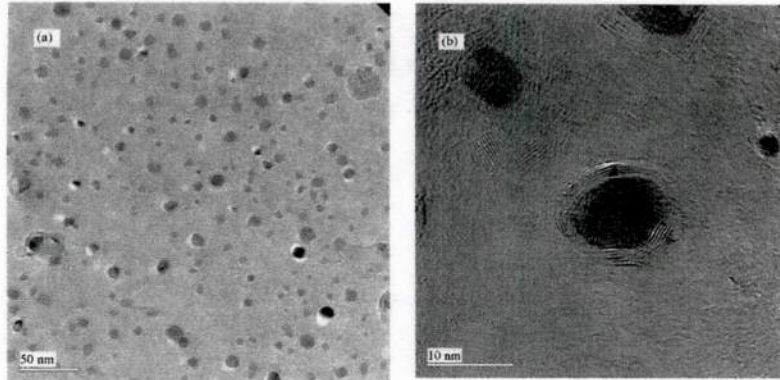


Figure 1. (Left) Low and (right) high resolution TEM images of the ceramic derived from a 2.6:1 weight ratio PND/PMCS blend pyrolyzed to 1300°C showing silicon-carbide crystallites embedded in an amorphous boron-carbon phase

Certain compositions of the PND/AHPCS derived ceramics exhibited significant oxidation resistance. For example as is shown in Fig. 2 (left), many of the 1650 °C ceramic chars derived from PND/AHPCS showed good oxidative resistance with the weights of chars **13** and **16**, obtained from the 0.22 PND/AHPCS and 1.21:1 PND/AHPCS blends, respectively, remaining essentially constant up to 1200 °C. Extended time oxidation studies at constant temperatures also revealed significant oxidative resistance. For example, as shown in Fig. 2 (right), after treatment with air for 325 min at 1200 °C the weight of char **13** decreased ~10%, but then remained constant. SEM studies of samples after the 1200 °C oxidations revealed smooth surfaces consistent with the formation of the glassy silica or silica/borosilicate coatings that have previously been proposed to provide oxidation barriers for silicon-carbide/boron-carbide materials.

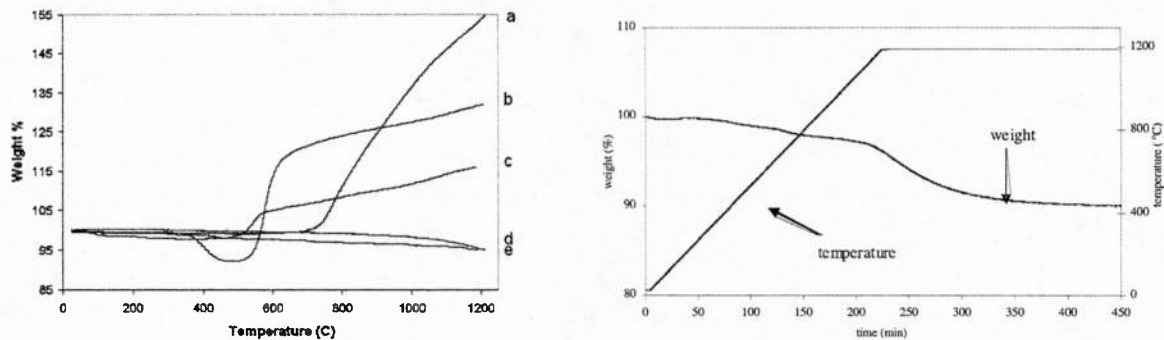


Figure 2. (Left) Overlap of TGA curves under dry breathing air of (a) commercial boron carbide, and the 1650 °C ceramic chars derived from (b) PND, (c) 2.63:1 PND/AHPCS, **21**, (d) 1.21:1 PND/AHPCS, **16**, and (e) AHPCS. (Right) TGA curve of char **13** (0.22 PND/AHPCS) under dry breathing air at 1200 °C (10 °C/min to 1200 °C, then held).

The PND/PMCS and PND/AHPCS blends now provide access to composite ceramics with different and controlled compositions and properties and, as illustrated by our oxidation and fiber-spinning studies (discussed in a later section), this flexibility can have significant advantages for the tuning of ceramic properties to fit the requirements for a range of potential applications.

A Simple Polymeric Precursor Strategy for the Syntheses of Complex Zirconium and Hafnium-Based Ultra High Temperature Silicon-Carbide Composite Ceramics

Hafnium and zirconium -borides, -carbides and -nitrides are chemically-inert, high-melting, extremely hard solids with high thermal stabilities.⁹ As a result, they are important high heat- and wear-resistant materials for use in severe environments, such as in nose and leading-edge applications in hypersonic aerospace vehicles where materials can be subjected to temperatures between 1600 and 2800 °C in an oxidizing environment of high velocity dissociated-air. Pure hafnium and zirconium -borides, -carbides and -nitrides form a protective metal-oxide scale under oxidizing environments, but the vaporization of other gaseous oxidation products (e.g., B₂O₃, CO₂, and NO₂, respectively) can increase the porosity of the surface layer and reduce the oxidation resistance of these materials. However, important recent work has shown that composite HfB₂/SiC and ZrB₂/SiC materials have significantly improved oxidative resistance compared to pure metal borides owing to the formation of a borosilicate-glass/metal-oxide surface scale which retards the B₂O₃ vaporization that would normally occur above 1600°C.¹⁰ Additionally, there is evidence that incorporating ZrC into the ZrB₂/SiC composite gives even greater protection against oxidation.¹¹

Metal-boride/silicon-carbide composites have previously been made by traditional powder methods, but these methods are limited in their ability to generate processed materials with controlled compositions and properties. A significant achievement¹² of this AFOSR project was the development of a simple chemical precursor strategy, employing metal dispersions in preceramic polymer blends, that has the potential to provide a wide range of new ultra high temperature zirconium and hafnium composite materials with tunable compositions, microstructures and/or stabilities.

The metal/PND/PMCS precursor blends were prepared by simply adding zirconium or hafnium metal to solutions of the polymer blends, followed by solvent evacuation with ultrasonic agitation to give the intimately mixed dispersion. XRD studies of the Zr/PND/PMCS dispersions heated at 1600 °C showed formation of zirconium-diboride/zirconium-carbide composites. The XRD studies (Figure 3) of the Hf/PND/PMCS sample heated at 1300 °C indicated complete consumption of the hafnium metal, with only HfB₂ diffraction evident at this temperature. Further production of hafnium boride and initial crystallization of hafnium carbide were observed when the sample was heated at 1600 °C for 2 h.

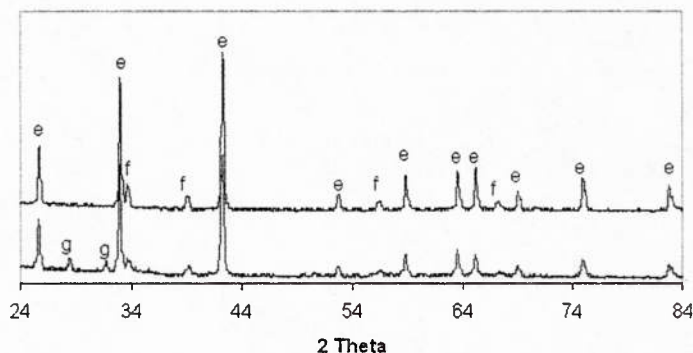


Figure 3. XRD analyses of ceramics derived from hafnium dispersed in a 1.8:1 weight ratio PND/PMCS blend following pyrolysis at 1300 °C (bottom) and 1600 °C (top). Diffraction peaks: (e) hafnium diboride; (f) hafnium carbide; (g) hafnium oxide.

While silicon-carbide composites containing hafnium and zirconium boride/carbide materials have been previously prepared by sintering powders at high temperatures, the silicon-carbide phases in these materials were highly crystalline. In contrast, no silicon carbide diffraction peaks were observed in the 1600 °C chars derived from the Zr/PND/PMCS and Hf/PND/PMCS dispersions. As shown in Figure 4 for a 1300 °C Hf/PND/PMCS char, TEM investigations of these materials suggest structures composed of metal-diboride and metal-carbide crystallites imbedded in an amorphous silicon carbon framework. EELS analysis confirmed the high silicon and carbon content of the amorphous phase.

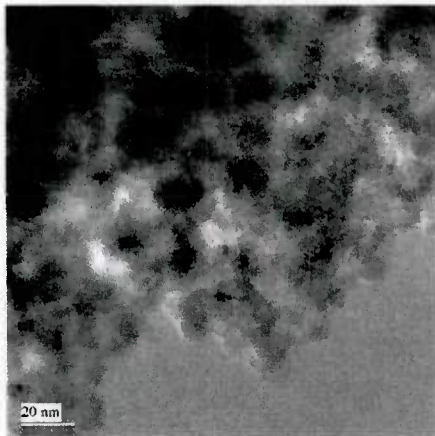


Figure 4. High resolution TEM analysis of the Hf/PND/PMCS blend pyrolyzed at 1300 °C showing hafnium diboride nanocrystallites embedded in an amorphous matrix

This polymer blend based route is thus unique in its ability to produce complex composites composed of an amorphous silicon-carbide matrix containing nano- to micro-meter scale metal diboride/carbide crystallites. Such blend-based precursor systems now offer a more systematic way to both generate more complex materials and tune the compositions and microstructures of the ceramic composites than can be attained by conventional powder methods. These results also suggest that blends of other preceramic polymers can likewise be used to produce arrays of new multiphase ceramic materials.

Electrostatic Spinning of Preceramic Polymer Blends to Produce Nano and Microscale Boron-Carbide/Silicon-Carbide Composite Fibers.

While electrostatic spinning¹³ of polymeric precursors has previously been shown to be an efficient and simple method to prepare fine fibers of many materials, our recent reports¹⁴ of the electrostatic spinning of the PND polymer and the subsequent conversion of the PND polymer fibers to boron-carbide/carbon fibers was the first use of this technique to prepare nonoxide ceramic fibers. In conjunction with Harry Allcock's group at Penn State, work completed in this AFOSR project demonstrated⁷ that 20 cm x 20 cm non-woven mats of PND/PMCS polymer composite fibers (Fig. 5a) could be readily obtained by the electrostatic spinning of THF solutions of the 1.2:1.0 and 2.6:1.0 PND/PMCS blends.

The pyrolytic ceramic conversion reactions of these PND/PMCS polymer fibers were then shown to produce mats of micro- and nano-diameter boron-carbide/silicon-carbide ceramic composite fibers. Thus, the SEM images (Figure 5) of mats of the ceramic fibers obtained from a 2.55:1 PND/PMCS blend by pyrolysis at (b) 1000 °C, (c) 1300 °C and (d) 1600 °C showed that

the fiber structure was been retained following ceramic conversion of the polymeric blend fibers (a).

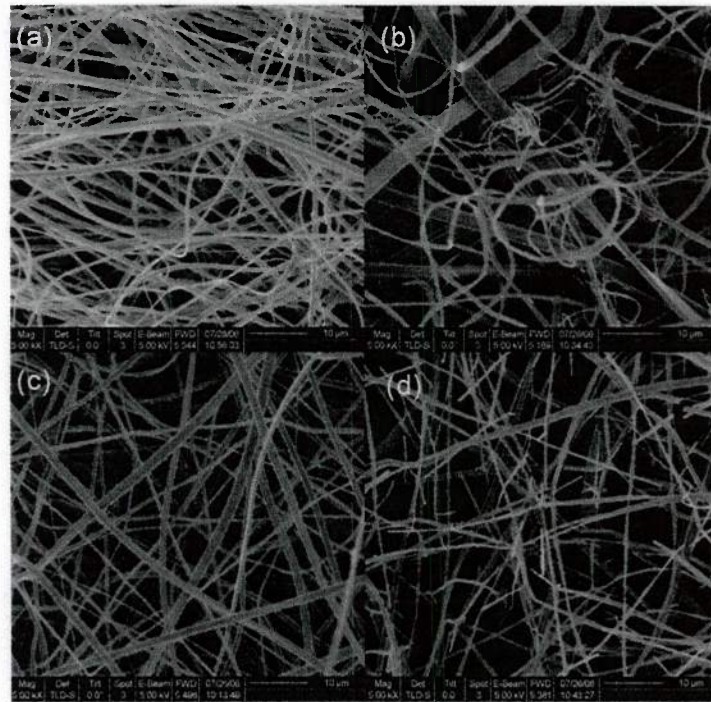


Figure 5. SEM images of fiber mats obtained from a 2.55:1 PND:PMCS blend polymer fibers (a), and the boron-carbide/silicon-carbide ceramic fibers obtained by pyrolysis at (b) 1000 °C, (c) 1300 °C and (d) 1600 °C.

As can be seen in the TEM images in Figure 6, the 1000 °C ceramic fibers had a smooth amorphous like surface structure, but that significant surface roughening occurred as the annealing temperature was increased to 1300 °C and 1600 °C. The XRD patterns of the composite ceramic fibers were found to closely match those obtained from the bulk ceramic conversions. For example, as can be seen in the XRD patterns in Figure 7, which were obtained from the 1300 °C chars of bulk chars and electrostatically-spun mats of a 2.6:1 PND/PMCS blend, both materials showed at this stage the formation of β -SiC crystallites, with the boron-carbide remained amorphous.

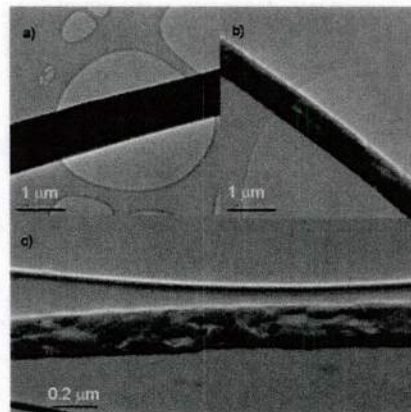


Figure 6. TEM images of 2.55:1 PND:PMCS fibers pyrolyzed to (a) 1000 °C, (b) 1300 °C, and (c) 1600 °C.

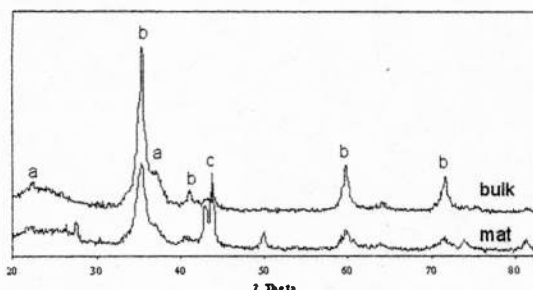


Figure 7. A comparison of the XRD patterns of the 1300 °C chars of the bulk (top), and electrostatically-spun polymer mats, (bottom), of a 2.55:1 PND/PMCS blend. Diffraction peaks: (a) boron carbide, (b) silicon carbide and (c) stainless steel holder.

Template-Based Precursors Routes to Micro- and Nano-Structured Nonoxide Ceramics

Silica Bead Templating

The design of solids with ordered macroporosities has recently received great attention because of the possibility that such materials could serve as photonic band gap and optical stop-gap materials,¹⁵ as well as catalyst supports and gas separation membranes. Although methods for producing ordered porous materials with pore diameters less than 10 nm are well developed, only recently have techniques for producing uniform macroporous (>25 nm) materials been reported. These methods generally involve the controlled growth of a matrix around an ordered array of macroscale templates. Silica spheres, latex beads and triblock copolymers have each been employed as templates. Once the matrix structure is formed, the templates are then removed by either chemical etching or thermal decomposition to leave a macroporously ordered inorganic solid. For example, latex beads have been used as templates to construct, via sol-gel condensations, ordered macroporous arrays of titania, zirconia, and alumina. Other work employing the silica templates has yielded macroporous carbons.

In this AFOSR project this templating technique was used to make macroporous nonoxide ceramic structures.¹⁶ A macro-ordered silica array was first generated by employing the method recently reported by Colvin and others.¹⁷ The open space in this framework was then filled with our 6,6'-(CH₂)₆-(B₁₀H₁₃)₂ boron-carbide¹⁸ or the commercial AHPCS silicon-carbide precursor by immersion in melts of the precursors.

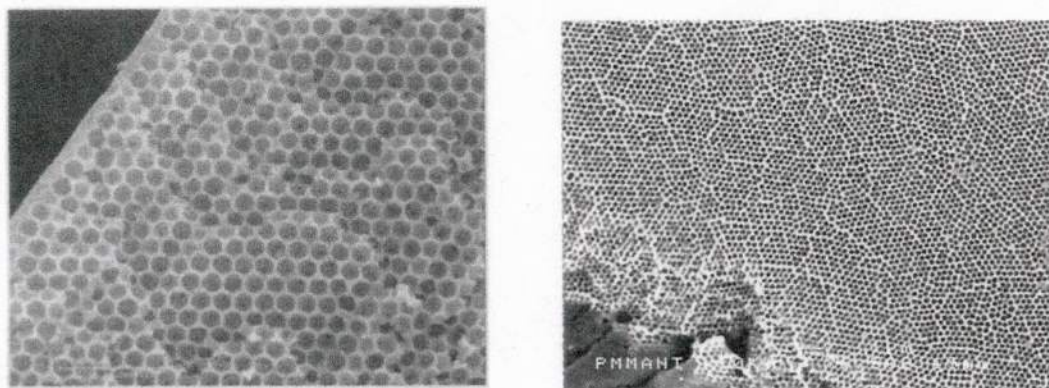


Figure 8. SEM images of nanoporous boron carbide (left) and silicon carbide (right) generated via silica bead templating of preceramic precursors.

Pyrolysis of the filled body to 1025°C, then yielded either a boron carbide or silicon carbide matrix surrounding the silica spheres. The silica spheres were then etched from the matrix by treatment with 48% HF to leave a “holey” ceramic framework. The SEM images in the Figure 8 show the ordered boron carbide (left) and silicon carbide arrays with ~50 nm pores that were achieved. These arrays can then be used to make more complex materials by filling in the holes in one ceramic array with a complimentary material to make, for example, ceramic-ceramic, ceramic-polymer, or ceramic-metal composite materials for structural, electronic and/or optical applications.

Diatom Templating

The potential applications of nanoporous ceramics require their large-scale production. However, the use of silica bead templating is scale-limited because of the tedious and time-consuming methods required for the generation of uniform silica beads. This need stimulated our interest in finding ways of achieving nanoporous ceramics more efficiently on much larger scales. Ken Sandhage at Georgia Tech has shown in a series of elegant papers¹⁹ that the microshells (frustules) of diatoms (a type of single-celled aquatic algae) can be used as templates for the formation of complex shapes of solid-state materials. The intricate shapes and fine features (i.e. nanopores, channels and protuberances) of the frustules are specific to each species of diatom. Because the formation of these shells is under genetic control, a given species produces replicas with a high degree of fidelity. The high continuous reproduction of the diatoms can yield enormous numbers of identically shaped frustule structures. As pointed out by Sandhage, such a genetically precise and massively parallel production is highly attractive means of producing large quantities of intricately nanostructured templates.

Sandhage already demonstrated¹⁹ that frustules can be used as templates for the formation of other materials, ranging from oxide ceramics to conventional organic polymers. However, before our recent AFOSR-sponsored work, there had been no previous use of these methods for the generation of nanostructured nonoxide ceramics. A collaboration with the Sandhage group combined our expertise in the design and properties of polymeric precursors to nonoxide ceramics with their expertise in growing and characterizing diatoms and diatom-templated materials and achieved^{16a,20} the use of these diatom-templating methods to generate nonoxide nanostructured materials on much larger scales than possible using man-made templates.

The SEM images below show the intricate structures of the *Aulacoseira* and *Nitzschia alba* frustules that were used in our studies.

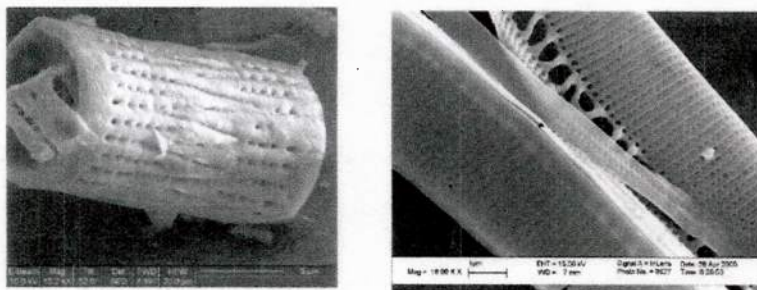


Figure 9. SEM images of the *Aulacoseira* (left) and *Nitzschia alba* (right) frustules

The templating procedure involved the initial treatment of the frustule with a solution of the preceramic precursor, evaporation of the solvent to leave a polymer-coated template, then

ceramic conversion at 800 °C to produce ceramic coated diatoms. This process is illustrated by the examples below in Figures 10-12 which employed our polyborazylene²¹ boron-nitride precursor.

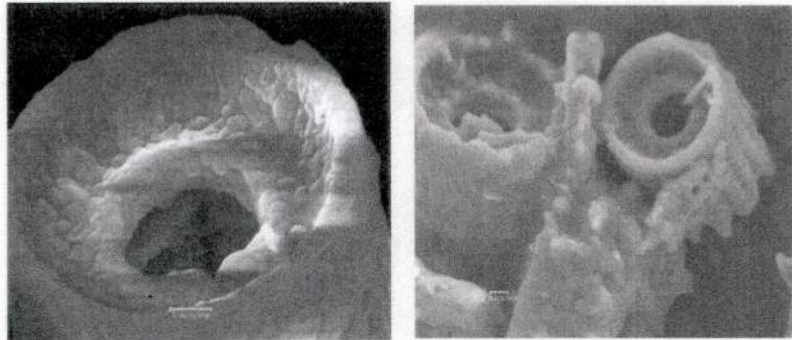


Figure 10. SEM Images of *Aulacoseira* Frustules Coated with Boron Nitride before Etching

The SEM images below show BN structures that were obtained from thickly coated frustules after etching with HF to remove the diatom silica substructure.

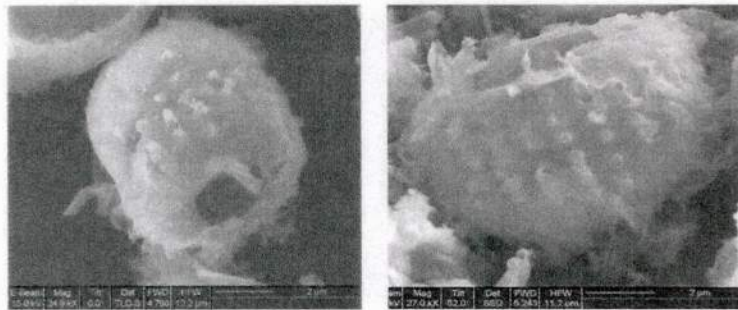


Figure 11. SEM Images of Boron Nitride Structures obtained after Etching of Coated *Aulacoseira* Frustules

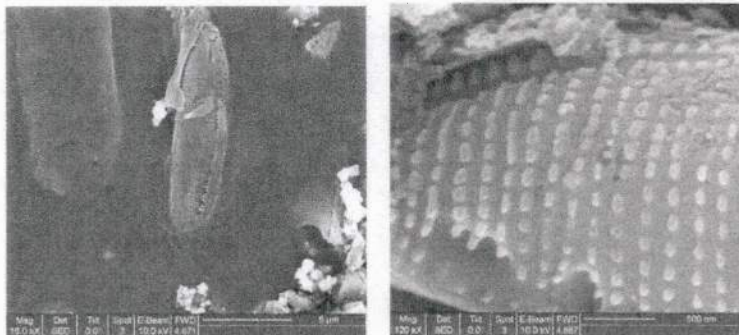


Figure 12. SEM Images of Boron Nitride Structures obtained after Etching of Coated *Nitzschia alba* Frustules

High-resolution TEM analyses of this particle clearly show the lattice fringes characteristic of turbostratic boron nitride.

We have also explored the potential applications of these nanostructured particles in ceramic-matrix and polymer-matrix composites to enhance properties, such as toughness or hardness. As shown in the SEM images below, pyrolysis of dispersions of the templated boron-nitride materials in the AHPCS polymer produced boron-nitride/silicon-carbide composites. Since the liquid AHPCS can fill the insides of the particles, they remained dispersed during ceramic conversion to produce homogeneous composites.

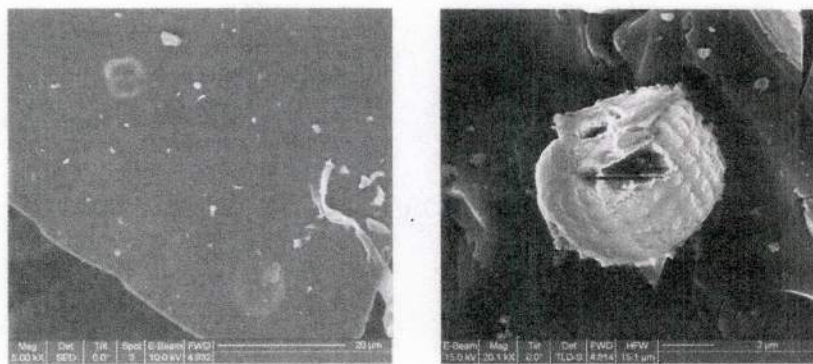


Figure 13. Backscattered and Secondary Electron Images Boron Nitride Templated Structures Dispersed in an AHPCS-Derived Silicon Carbide Matrix Fired to 1650 °C

Fabrication of High Temperature Ceramic Photonic Crystals

In the last year of this grant, new studies exploiting the complementary expertise of the research groups of Larry Sneddon (Chemistry) in ceramic precursor synthesis/properties and Shu Yang (Materials Science) in state-of-the-art nano- and microfabrication methods achieved the construction of photonic crystals based on high temperature ceramic materials.²²

The Yang lab fabricated the 3D diamond-like template structures that were needed for the fabrication of 3D ceramic photonic crystals from photopatternable epoxy-cyclohexyl polyhedral oligomeric silsesquioxanes (POSS) using multi-beam interference lithography (see Fig. 14a).²³ The POSS films were found to be thermally and mechanically stable up to 350 °C (Fig. 14b). At and above 400 °C in air, however, micro-cracks occurred throughout the film due to large mass loss and mismatch of coefficient of thermal expansion (CTE) with the substrate (e.g. Si) (Fig. 14c). In contrast, the film remained crack-free after O₂ plasma treatment (Fig. 14d-e) or calcination in Ar. At longer plasma etching times, the porosity was further increased, which should allow the manipulation of the filling fraction to maximize the bandgap width.

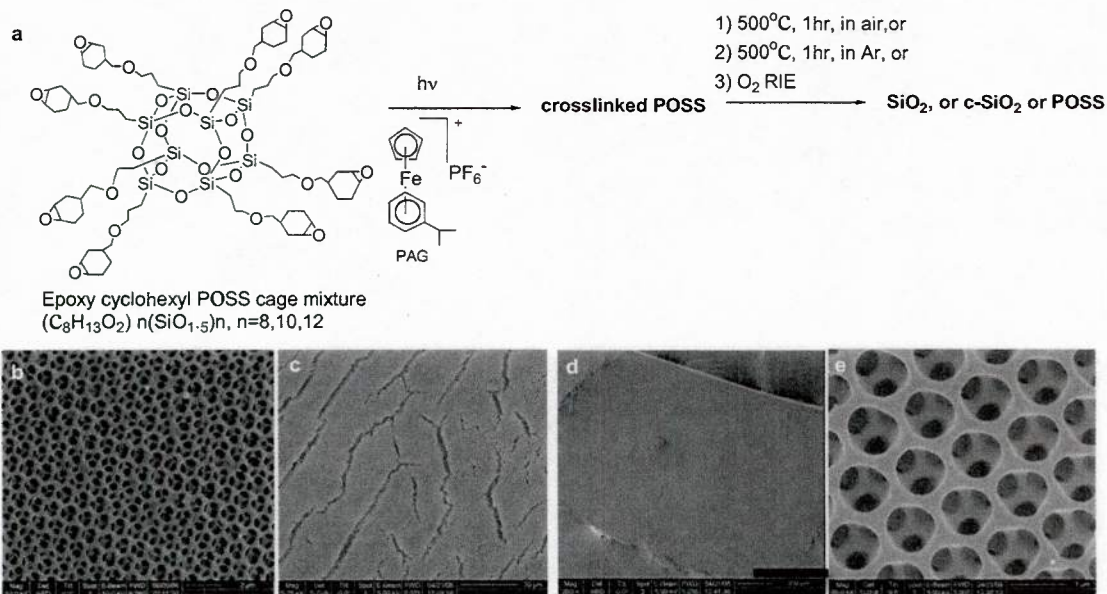


Figure 14. Diamond-like POSS structures treated at different conditions. a) Schematics of the chemistry and process. b-e) SEM images of POSS structures after b) 320 °C for 1hr in air, c) 500 °C for 1hr in Air, and d-e) O₂ plasma for 1hr at 30W.

FTIR spectra and energy-dispersive X-ray spectroscopy (EDX) studies suggest that the films were toughened by the introduction of carbon. EDX shows that the elemental composition of the O₂ plasma treated film (for a short period of time, e.g. 1hr) is nearly identical to that of epoxy POSS film (Fig. 15). While only trace carbon is left in the film treated in air, a large quantity of *sp*³ carbon appeared in the film that was heated in only Ar.

Pre-ceramic silicon carbide polymers from the Sneddon group were then used to fill these 3D templates. Ceramic conversions at 1100 °C followed by the removal of the silica templates with HF etching, then resulted in the formation of inverse photonic crystal ceramics, such as the 3D-structured SiC and B₄C shown in Figure 16. The quality of 3D ceramic crystals was found to be highly dependent on the quality of POSS template. As seen in Fig. 16b, when the SiC 3D crystal was templated from POSS calcined at 500 °C in air (Fig. 14b), the ceramic conversion at 1100 °C increased the micro-crack formation (Fig. 16b). In contrast, many fewer cracks were observed in SiC crystals that were templated directly from the crack-free POSS structures after treatment at 1100 °C in Ar (Fig. 16c). Templated crack-free ceramic samples can now be obtained over a large area (~500 μm). The success of these initial studies now indicates that a wide variety of 3D-structured high temperature ceramic materials, over a range of nano to micro length scales, should be attainable using these template methods. Following the same processing procedure, we fabricated 3D boron carbide photonic crystals. Likewise, many fewer cracks were observed in B₄C 3D structures templated directly from POSS.

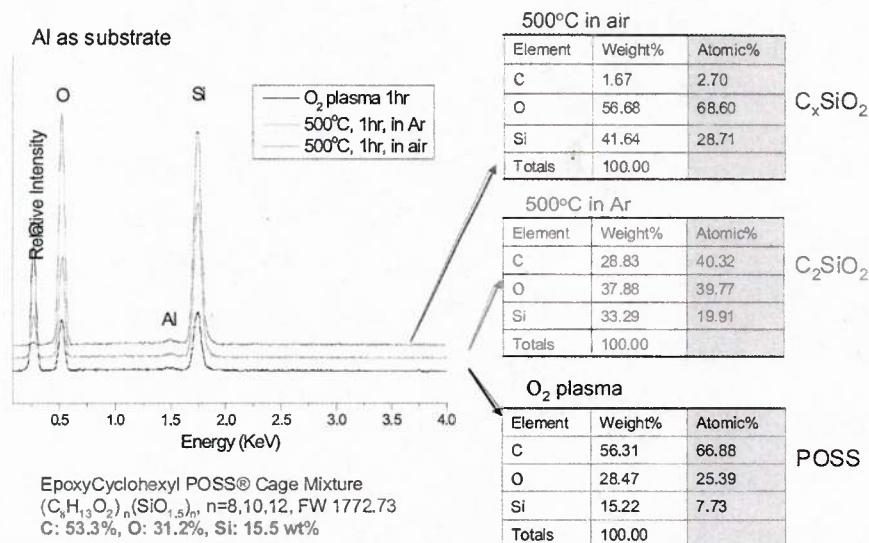


Figure 15. Elemental analysis of 3D epoxy POSS films treated at different conditions by EDX.

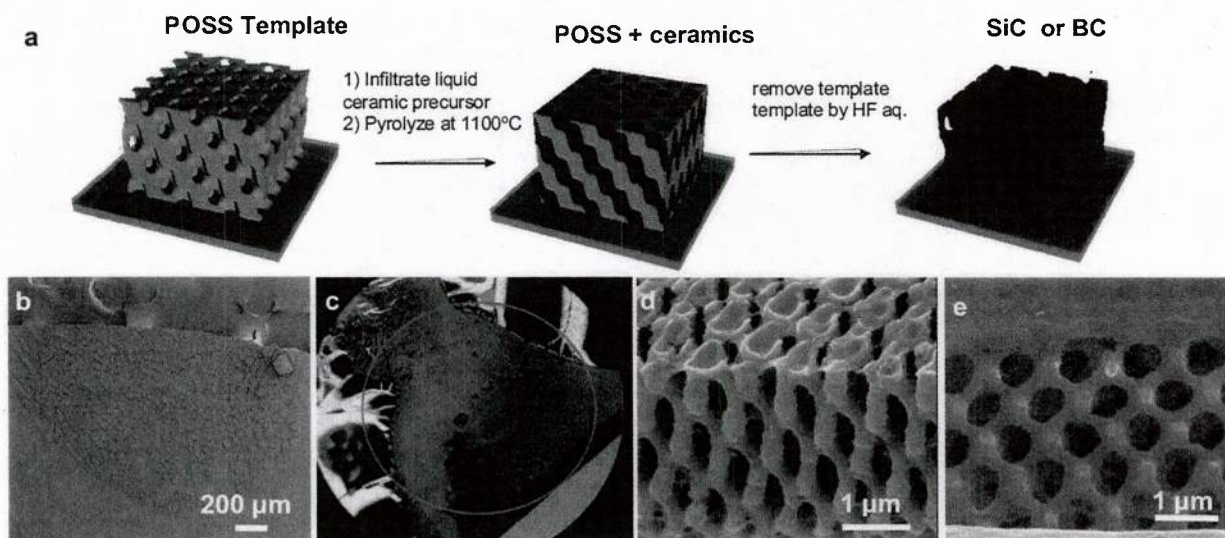


Figure 16. Diamond-like ceramic photonic crystals. (a) Schematics of the fabrication process. (b) SEM image of SiC templated from 3D POSS structure calcined in air at 500°C. (c) Optical image of SiC templated directly from 3D POSS structure, followed by heat treatment at 1100°C in Ar for 2hrs. (d-e) SEM images of inverse 3D SiC (d) and B₄C (e) 3D photonic crystals obtained from direct backfilling of POSS template.

We are optimizing the fabrication procedures and extending these methods to other preceramics/ceramics. In addition, we have started to quantitatively evaluate the corresponding photonic bandgap properties of these new materials by using FT-IR to measure the reflectance of the 3D photonic crystals, including: (1) the POSS template; (2) backfilled POSS/ceramic composite; and (3) the inversed ceramics obtained at different processing steps, for comparisons with their calculated photonic band gaps (PBGs). As seen in Fig. 17, a stop band peak at 1.78 μm was observed from the 3D POSS template. In the SiC/template composite, there was a bathochromic shift of the reflection peak to ~ 2.45 μm. This was due to the increase of mean refractive index of SiC/template structure. After removal of the template, a blue shift of stop

band to $1.84 \mu\text{m}$ was observed for the inverse SiC 3D structure since the mean refractive index was decreased. We note that the peak reflectivity increased significantly from 0.8 (3D POSS) to 2.0 (inverse 3D SiC), indicating increased optical quality of the films.

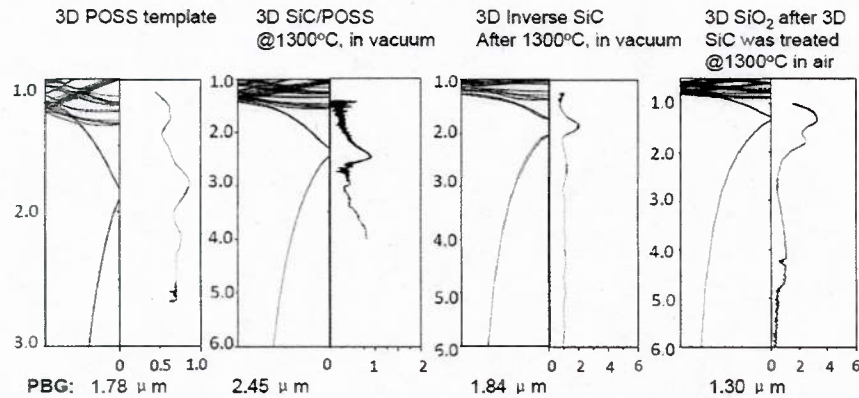


Figure 17. FTIR reflectance spectra of 3D diamond-like structures processed at different stages in the [111] direction. In each panel, the left figure is a simulated spectrum and the right one is the experimental FTIR spectrum.

In order to determine the potential of these 3D ceramic crystals for high temperature applications under oxidizing conditions, we performed thermal gravimetric analyses (TGA) of these materials to $1100 \text{ }^\circ\text{C}$ under vacuum and air environment for 1hr. As seen in Fig. 18, the 3D SiC structure was well-maintained after exposure to $1100 \text{ }^\circ\text{C}$ under vacuum: only a small shrinkage, 3.8% and 3.3% in the (111) plane and [111] direction, respectively, was observed compared to the 3D SiC crystal before the additional sintering at $1100 \text{ }^\circ\text{C}$ under vacuum. Further heating to $1300 \text{ }^\circ\text{C}$ under vacuum showed almost no shrinkage of the 3D structures. However, when heated in air, both at 1100 and $1300 \text{ }^\circ\text{C}$ for 1hr, the 3D SiC was completely oxidized to SiO_2 while the 3D structure was maintained, with a photonic bandgap at $1.30 \mu\text{m}$.

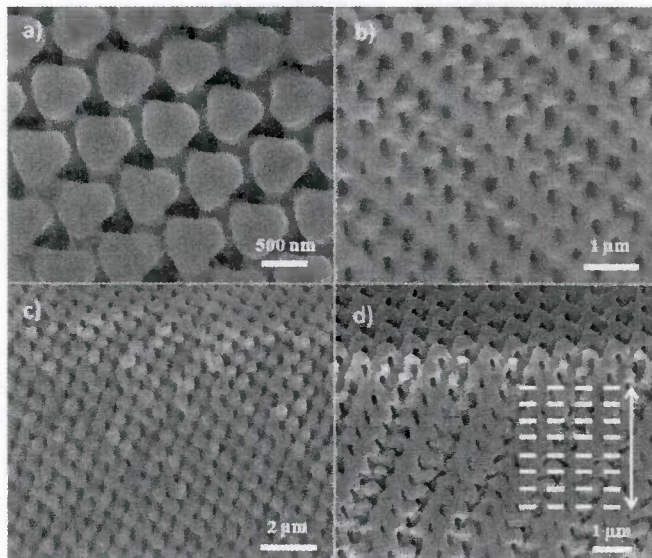


Figure 18. SEM images of inverse diamond-like SiC photonic crystals pyrolyzed at $1100 \text{ }^\circ\text{C}$ under vacuum for 1hr with a heating rate of $3 \text{ }^\circ\text{C}/\text{min}$: (a) Overview, (b) Top view, (b, c) Cross-sectional views in different plane directions. (d) Cross-sectional view of the sample FIB milled in perpendicular to the (111) plane and sample tilt at 52° .

Personnel Supported

Larry G. Sneddon	Blanchard Professor, University of Pennsylvania
Upal Kusari	Chemistry Graduate Student, University of Pennsylvania
Marta Guron	Chemistry Graduate Student, University of Pennsylvania
Shahana Chatterjee	Chemistry Graduate Student, University of Pennsylvania
Yongan Xu	Materials Science Graduate Student, University of Pennsylvania
Guan-quan Liang	Materials Science postdoc, University of Pennsylvania

Publications Acknowledging AFOSR Support (2006-present)

1. X. Wei, P. J. Carroll and L. G. Sneddon, Ruthenium Catalyzed Ring Opening Polymerization Syntheses of Poly(organodecaboranes): New Single-Source Boron Carbide Precursors, *Chemistry of Materials*, 2006, 18: 1113-1123.
2. U. Kusari, Z. Bao, C. Ye, G. Ahmad, K. H. Sandhage and L. G. Sneddon, Template Routes to Non-Oxide Ceramic Nano- and Micro-Structures, *Materials Research Society Proceedings*, 2006, 921, T04-10.
3. U. Kusari, Z. Bao, C. Ye, G. Ahmad, K. H. Sandhage and L. G. Sneddon, Formation of Nanostructured, Nanocrystalline Boron Nitride Microparticles with Diatom-Derived 3-D Shapes, *Journal of the Chemical Society, Chemical Communications*, 2007, 1177-1179.
4. M. M. Guron, M. J. Kim and L. G. Sneddon, A Simple Precursor Strategy for the Syntheses of Complex Zirconium and Hafnium-Based Ultra High Temperature Silicon-Carbide Composite Ceramics, *Journal of the American Ceramic Society*, 2008, 91:1412-1415.
5. M. M. Guron, X. Wei, D. Welna, N. Krogman, M. J. Kim, H. Allcock and L. G. Sneddon, Pre-ceramic Polymer Blends as Precursors for Boron-Carbide/Silicon-Carbide Composite Ceramics and Ceramic Fibers, *Chemistry of Materials* 2009, 21:1708-1715.
6. J. Moon, J. S. Seo, Y. Xu, and S. Yang, Direct fabrication of 3D silica-like microstructures from epoxy-functionalized polyhedral oligomeric silsesquioxane (POSS), *Journal of Materials Chemistry* 2009, 19: 4687-4691.
7. Y. Xu, M. Guron, X. Zhu, L. G. Sneddon, and S. Yang, 3D Non-oxide Ceramic Photonic Crystals for Ultra High Temperature Applications, in preparation.

Acknowledgment/Disclaimer

This work was sponsored in part by the Air Force Office of Scientific Research, USAF, under grant number FA9550-06-1-0228. The views and conclusions contained herein are those of the authors and should not be interpreted as necessarily representing the official policies or endorsements, either expressed or implied, of the Air Force Office of Scientific Research or the U.S. Government.

References

1. (a) Messier, D. R.; Scroft, W. J. *Preparation and properties of solid state materials*, Wilcox, W. R. Ed.; M. Dekker: New York, 1976. (b) Narula, C. K. *Ceramic precursor technology and its applications*; M. Dekker: New York, 1995.
2. Thevenot, F. *Key Eng. Mater.* 1991, 56-57, 59-88.
3. (a) Shipilova, L. A.; Petrovskii, V. Y.; Chugunova, S. I. *Powder Metall. Met. Ceram.* **1998**, 36, 652-656. (b) Narushima, T.; Goto, T.; Maruyama, M.; Arashi, H.; Iguchi, Y. *Mater. Trans.* **2003**, 44, 401-406.
4. Guo, Q.; Song, J.; Liu, L.; Zhang, B. *Carbon* **1999**, 37, 33-40.
5. Kobayashi, K.; Maeda, K.; Sano, H.; Uchiyama Y. *Carbon* **1995**, 33, 397-403.
6. (a) Thummler, F.; Oberacker, R. *An introduction to powder metallurgy*, Institute of Materials: London, 1993. (b) Singh, M. *Scr. Mater.* **1996**, 34, 923-927. (c) Chen, Z. F.; Su, Y. C.; Cheng, Y. B. *Key Eng. Mater.* **2007**, 352, 207-212.
7. Guron, M. M. Wei, X.; Welna, D.; Krogman, N.; Kim, M. J.; Allcock, H.; Sneddon, L. G. *Chem. Mater.* **2009**, 21, 1708-1715.
8. (a) Wei, X.; Carroll, P. J.; Sneddon, L. G. *Organometallics* **2004**, 23, 163-165. (b) Wei, X.; Carroll, P. J.; Sneddon, L. G. *Chem. Mater.* **2006**, 18, 1113-1123.
9. Fahrenholtz, W. G.; Hilmas, G. E.; Talmy, I. G.; Zaykoski, J. A. *J. Am. Ceram. Soc.* **2007**, 90, 1347-1364 and references therein.
10. (a) Kuriakose, A. K.; Margrave, J. L. *J. Electrochem. Soc.* **1964**, 111, 827-831. (b) Matsushita, J.; Endo, T. *J. Adv. Sci.* **1998**, 10, 94-96. (c) Wuchina, E. J.; Opeka, M. M. *Electrochem. Soc. Proc.* **2001**, 12 136-143. (d) Metcalfe, A. G.; Elsner, N. B.; Allen, D. T.; Wuchina, E.; Opeka, M.; Opila, M. *Electrochem. Soc. Proc.* **2000**, 99-38, 489-501.
11. Monteverde, F.; Scatteia, L. *J. Am. Ceram. Soc.* **2007**, 90, 1130-1138.
12. Guron, M. M.; Kim, M. J.; Sneddon, L. G. *J. Amer. Cer. Soc.* **2008**, 91, 1412-1415.
13. For general references on the use of electrostatic spinning to produce ceramic fibers, see (a) Fong, H. In *Polymeric nanostructures and their applications*; Nalwa, H. S., Ed.; Am. Sci. Pub.: Stevenson Ranch, Calif., 2007; Vol 2, p. 451-474. (b) Ramaseshan, R.; Sundarajan, S.; Jose, R.; Ramakrishna, S. *J. Appl. Phys.* **2007**, 102, 111101/1-111101/17. (c) Li, D.; McCann, J. T.; Xia, Y.; Marquez, M. *J. Am. Ceram. Soc.* **2006**, 89, 1861-1869. (d) Sigmund, W.; Yuh, J.; Park, H.; Maneeratana, V.; Pyrgiotakis, G.; Daga, A.; Taylor, J.; Nino, J. C. *J. Am. Ceram. Soc.* **2006**, 89, 395-407.
14. (a) Welna, D. T.; Bender, J. D.; Wei, X.; Sneddon, L. G.; Allcock, H. R. *Adv. Mater.* **2005**, 17, 859-862. (b) Welna, D. T.; Wei, X.; Bender, J. D.; Krogman, N.R.; Sneddon, L. G.; Allcock, H. R. *Mater. Res. Soc. Proc.* **2005**, 848, 287-292.
15. Polman, A.; Wiltzius, P., *MRS Bull.* **2001**, 26, 608.
16. (a) Kusari, U.; Bao, Z.; Ye, C.; Ahmad, G.; Sandhage, K. H.; Sneddon, L. G. *Mater. Res. Soc. Proc.*, **2006**, 921, T04-10. (b) Sneddon, L. G.; Pender; M. Forsthoefel, K.; Kusari, U.; Wei, X. *J. Eur. Ceram. Soc.* **2005**, 25, 91-97.
17. (a) Jiang, P.; Bertone, J. F.; Hwang, K. S.; Colvin, V. L., *Chem. Mater.* **1999**, 11, 2132. (b) Jiang, P.; Hwang, K. S.; Mittleman, D. M.; Bertone, J. F.; Colvin, V. L., *J. Am. Chem. Soc.* **1999**, 121, 11630. (c) Stöber, W.; Fink, A.; Bohn, E., *J. Colloid Interface Sci.* **1968**, 26, 62. (d) Turner, M. E.; Trentler, T. J.; Colvin, V. L., *Adv. Mater.* **2001**, 13, 180.

18. Pender, M. J.; Carroll, P. J.; Sneddon, L. G. *J. Am. Chem. Soc.* **2001**, *123*, 12222-12231.
19. (a) Dickerson, M. B.; Naik, R. R.; Sarosi, P. M.; Agarwal, G.; Stone, M. O.; Sandhage, K. H. *J. Nanosci. Nanotechnol.* **2005**, *5*, 63. (b) Gaddis, C. S.; Sandhage, K. H. *J. Mater. Res.* **2004**, *19*, 2541. (c) Sandhage, K. H.; Dickerson, M. B.; Huseman, P. M.; Caranna, M. A.; Clifton, J. D.; Bull, T. A.; Heibel, T. J.; Overton, W. R.; Schoenwaelder, M. E. A. *Adv. Mater.* **2002**, *14*, 429. (d) Unocic, R. R.; Zalar, F. M.; Sarosi, P. M.; Cai, Y.; Sandhage, K. H. *Chem. Commun.* **2004**, *7*, 796. (e) Weatherspoon, M. R.; Allan, S. M.; Hunt, E.; Cai, Y.; Sandhage, K. H., *Chem. Commun.* **2005**, 651. (f) Zhao, J. P.; Gaddis, C. S.; Cai, Y.; Sandhage, K. H. *J. Mater. Res.* **2005**, *20*, 282.
20. Kusari, U.; Bao, Z.; Ye, C.; Ahmad, G.; Sandhage; K. H.; Sneddon, L. G. *Chem. Commun.* **2007**, 1177-1179.
21. (a) Fazen, P. J.; Beck, J. S.; Lynch, A. T.; Remsen, E. E.; Sneddon, L. G. *Chem. Mat.* **1990**, *2*, 96. (b) Fazen, P. J.; Remsen, E. E.; Beck, J. S.; Carroll, P. J.; McGhie, A. R.; Sneddon, L. G. *Chem. Mat.* **1995**, *7*, 1942.
22. Xu, Y. Guron, M. M.; Zhu, X.; Sneddon, L. G.; Yang, S. in preparation.
23. Moon, J.; Seo, J. S.; Xu, Y.; Yang, S. *J. Mater. Chem.* **2009**, *19*, 4687-4691.